Flux Weakening Strategy of an Induction Machine Driven by an Electrolytic Capacitor-less Inverter

Anno Yoo
Student Member, IEEE
Seoul National University
Seoul, Korea
realanno@eepel.snu.ac.kr

Seung-Ki Sul
Fellow, IEEE
Seoul National University
Seoul, Korea
sulsk@plaza.snu.ac.kr

Sunja Kim
LS Industrial System Co,
Anyang-si, Gyeong, Korea
Sjkim3@lsis.biz

Kyung-Seo Kim
Member, IEEE
LS Industrial System Co,
Anyang-si, Gyeong, Korea
kyungseok@lsis.biz

***Abstract* -- This paper presents a novel flux weakening strategy of an induction machine driven by an electrolytic capacitor-less inverter. In the electrolytic capacitor-less inverter, the DC-link voltage is fluctuating at six times of frequency of input three phase source due to its small DC-link capacitance. Hence, the decoupling of the fluctuation and maximum utilization of the DC-link voltage is the major issue in the electrolytic capacitor-less inverter. In this paper, the cost function is set to increase the voltage utilization of the inverter for the flux weakening operation of an induction machine. By the proposed cost function and flux weakening strategy, the operating speed of the induction machine is extended above base speed without any stability problem. The experimental results show the effectiveness of proposed strategy.**

***Index Terms*—electrolytic capacitor-less inverter, induction machine, flux weakening operation**

I. INTRODUCTION

Recently, the size and cost of reactive components such as inductors and electrolytic capacitors is one of the main concerns in the design of DC-link based AC-DC-AC power converters. Especially, the large electrolytic capacitors in the DC-link, whose life expectancy is usually shorter than any other components in the converters, are bulky and expensive [1]. Also, the additional pre-charging circuit is necessary to reduce the inrush current to the large capacitor bank. Although the pre-charging time is very short compared to the total operation periods, the cost and volume of the circuit is not negligible.

Due to the above issues, there have been many researches to reduce the DC-link capacitance [2]-[7]. With the reduced DC-link capacitor, Total Harmonic Distortion (THD) of input current can be improved, and the total volume and the cost also can be reduced.

There are several types of the reduced DC-link capacitance Voltage Source Inverter (VSI). The converter proposed in [3] uses the Diode Front-End (DFE) rectifier and the reduced DC-link capacitor. By using DFE rectifier, the inverter can operate only in the motoring mode. In [4]-[5], the Active Front-End (AFE) rectifier which is identical to the PWM boost converter with reduced DC-link capacitor was introduced. Although its input current is almost sinusoidal, it is required to install the large inductors for the PWM boost converter, which possibly increase the volume and the cost. And, the size of DC-link capacitance is dependent on the load power. That is, higher load power demands larger DC-link capacitance. In [6], the PWM boost converter using the small DC-link capacitor whose value is independent on the load power had been demonstrated. However, its performance is sensitive to the parameters variation. In [2] and [10], the electrolytic capacitor-less inverter with bi-directional rectifier is presented. Although the input filter should be installed, the inductance of input filter is quite small compared to PWM boost converter and this power converter can be operated both in motoring and regenerating modes due to its bi-directional rectifier. With above advantages, this power converter is incorporated with the proposed flux weakening algorithm in this paper.

However, in the above mentioned previous researches, the main focus is on the constant torque region operation of the induction machine. There had been several preferred approaches that enhance the flux weakening performance of an induction machine. In [7], the simple flux weakening operation was proposed when using the electrolytic capacitor-less inverter with DFE rectifier. In this method, however, the maximum steady state output voltage is limited to the minimum DC-link voltage and the available voltage to the induction machine is restricted within the linear modulation region. In [8], the maximum torque control of an induction machine in the flux weakening region was introduced. However, this method depends on the machine parameters and does not consider the fluctuation of DC-link voltage. Hence, its performance is limited and may be degraded in over all operating conditions especially in case of electrolytic capacitor-less inverter, where the DC link voltage is fluctuating. In [9], the rotor flux reference varies according to the speed, which is a commonly used flux weakening method of an induction machine. However, this method can not obtain the maximum torque as mentioned in [8].

In this paper, a novel flux weakening operation for an induction machine is presented, driven by an electrolytic capacitor-less inverter which is presented in [2] and [10]. The proposed flux weakening strategy increases the voltage utilization under the continuous fluctuation of DC-link voltage due to the small capacitance in the DC-link. Based on the cost function, DC-link voltage can be utilized maximally in the flux weakening operation region. The experimental results show the effectiveness of the proposed flux weakening method.

II. ANALYSIS OF ELECTROLYTIC CAPACITOR-LESS INVERTER WITH BI-DIRECTIONAL RECTIFIER

Fig. 1 shows the block diagram of the electrolytic capacitor-less inverter addressed in this paper. As shown in Fig. 1, there is only a several μF film capacitor in the DC-link. That is, there is no inductor and braking chopper in the DC-link. However, an input filter is required to smooth the input current in the electrolytic capacitor-less inverter because the most of PWM switching ripples of the inverter currents would transfer to the input source due to small capacitance in the DC-link. Considering the cost and the volume, LC or LCL filter with damping resistor can be a candidate of an input filter. In this paper, a simple LC filter with damping resistor is used as the input filter.

Fig. 2 demonstrates the experimental results of the input current and its frequency spectrum at 4kW motoring mode in case of 380V_{rms} line-to-line input voltage. With the small DC-link capacitance, the input 'a' phase current is quasi-square wave as shown in Fig.2(a) and 5th and 7th harmonic current is below 15%. Hence, THD of input current is below 25%.

Also, the DC-link voltage has the inevitable fluctuation whose frequency is 6 times of line frequency due to the small DC-link capacitance. In the DC-link voltage, the maximum and minimum value is governed by the input line-to-line voltages as (1) and (2).

$$V_{dc\_\max} = \max\left(\sqrt{2}\, v_{line-to-line}\right) \quad (1)$$

$$V_{dc\_\min} = \max\left(\sqrt{2}\, v_{line-to-line}\right) \cos\left(\frac{\pi}{6}\right) \quad (2)$$

where $v_{line-to-line}$ is the input line-to-line voltage in r.m.s., $V_{dc\_\max}$ is the maximum DC-link voltage, and $V_{dc\_\min}$ is the minimum DC-link voltage.

As shown in (1) and (2), the minimum DC-link voltage is 86.6% of maximum one theoretically. However, DC-link voltage can be varied according to the operation mode because of the effect of input filter [10]. Especially, the minimum DC-link voltage at the motoring mode is much lower than one at the regenerating mode. Hence, it is important to decide how to synthesize output voltage of the inverter under this fluctuating DC-link voltage.

In Fig.1, it can be understood that the switching frequency of the bi-directional rectifier is the same to the frequency of the input line voltage. Although the structure is similar to the PWM boost converter, the switching instance of converter is synchronized with the parallel diode commutation. And, the operation of the bi-directional rectifier has nothing to do with the operation of the PWM inverter part. Fig. 3 shows the block diagram of the converter switching instant according to the line-to-line input voltage. As shown in Fig. 3, as the switching frequency is equal to the input line frequency, the switching loss is significantly reduced compared to the PWM boost converter. As a result, it is not necessary to install an additional heat sink and pre-charging circuit which are burden to PWM boost converter. Also, the regenerating

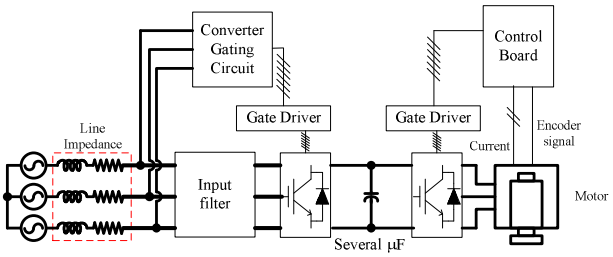

Fig. 1 Block diagram of electrolytic capacitor-less inverter

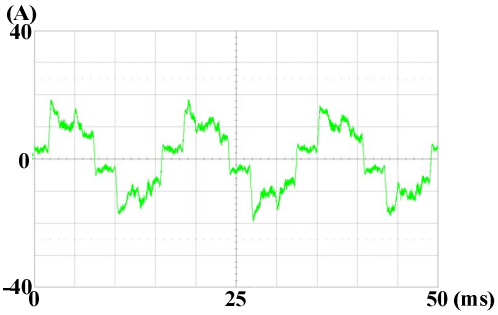

(a) Input 'a' phase current

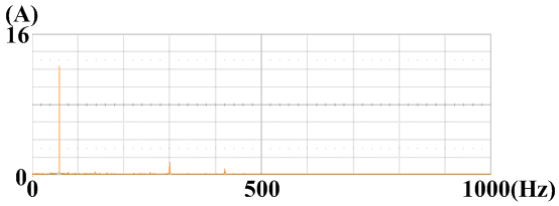

(b) FFT of input current

Fig. 2 Input current and FFT of input current at 4kW motoring

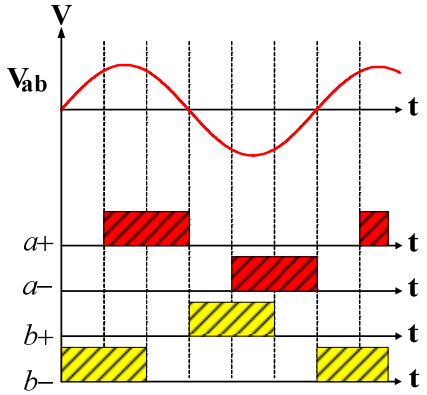

Fig. 3 switching sequence of bidirectional rectifier according to input line-to-line voltage

(Vab : 'ab' line-to-line voltage, a+ : 'a' phase upper switch, a- : 'a' phase lower switch, b+ : 'b' phase upper switch, b-: 'b' phase lower switch of the rectifier)

operation is possible owing to the inherent bi-directional power flow capability of the converter.

Fig. 4 demonstrates the experimental results when the 7.5kW induction machine driven by the electrolytic capacitor-less inverter is running in motoring mode and regenerating mode. In Fig.4, 'Ia' is the 'a' phase input current and 'Ea' is the 'a' phase input voltage. As shown, the

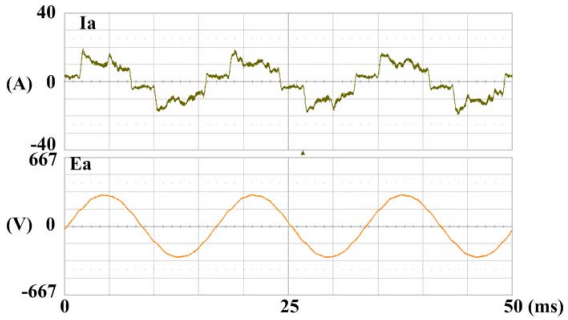

(a) 4kW motoring mode

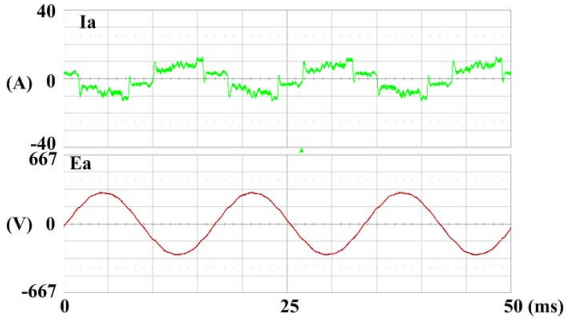

(b) 3kW regenerating mode

Fig. 4 Input current and FFT of input current at 4kW motoring

displacement power factor is almost 1.

III. Flux Weakening Operation of Induction Machine with Electrolytic Capacitor-less Inverter

As the speed increase, Back-EMF of an induction machine is grown up and the flux weakening operation should be applied to regulate the torque of the motor. Normally, the developed output torque in the flux weakening region is limited by both the current and DC-link voltage rating of inverter. As mentioned in Section II, the voltage margin in the electrolytic capacitor-less inverter is reduced compared to that in the conventional PWM VSI [11]. Hence, when using the electrolytic capacitor-less inverter, the base speed should be reduced appropriately.

The voltage equation of induction machine in the synchronous reference frame is given as (3) and (4).

$$v_{ds}^{e} = R_s i_{ds}^{e} + \sigma L_s \frac{d i_{ds}^{e}}{d t} + \frac{L_m}{L_r}\frac{d\lambda_{dr}^{e}}{d t} - \omega_e \sigma L_s i_{qs}^{e} \tag{3}$$

$$v_{qs}^{e} = R_s i_{qs}^{e} + \sigma L_s \frac{d i_{qs}^{e}}{d t} + \frac{L_m}{L_r}\omega_e \lambda_{dr}^{e} + \omega_e \sigma L_s i_{ds}^{e} \tag{4}$$

where v_{ds}^{e}, v_{qs}^{e}, i_{ds}^{e}, and i_{qs}^{e} stands for d and q-axis voltage and current in the synchronous reference frame, R_s for the stator resistance, L_s for stator self inductance L_r for rotor self inductance, L_m for mutual inductance, λ_{dr}^{e} for rotor flux in the synchronous reference frame, ω_e for operating frequency, and σL_s for stator transient inductance $\left(\sigma L_s = L_s - \frac{L_m^2}{L_r}\right)$, respectively.

In the steady state, the flux and the current in the synchronously rotating reference frame can be considered as constant. Because the voltage drop by the stator resistance is quite small compared to other terms in (3) and (4) in the flux weakening region, the voltage drop can be neglected in the region. From the above assumptions, the voltage equation in the synchronous reference frame can be approximated as (5) and (6).

$$v_{ds}^{e} \cong -\omega_e \sigma L_s i_{qs}^{e} \tag{5}$$

$$v_{qs}^{e} \cong \frac{L_m}{L_r}\omega_e \lambda_{dr}^{e} + \omega_e \sigma L_s i_{ds}^{e} = \omega_e L_s i_{ds}^{e} \tag{6}$$

And the developed torque in the steady state can be expressed as (7).

$$T_e = \frac{3}{2}\frac{P}{2}\frac{L_m}{L_r}\lambda_{dr}^{e} i_{qs}^{e} \tag{7}$$

where T_e is the generated torque and P is the number of poles.

There are two constraints in the flux weakening operation, one is the voltage limit and the other is the current limit.

First, the voltage limit is considered. The maximum stator voltage, $V_{s\_\max}$, is determined by the DC-link voltage, V_{dc} and PWM strategy. The voltage limit condition can be formulated as (8).

$$v_{ds}^{e\,2} + v_{qs}^{e\,2} \le V_{s\_\max}^{\;2} \tag{8}$$

From (5), (6), and (8), the voltage limit constraint can be expressed in terms of currents in the synchronous reference frame as (9).

$$\left(\omega_e \sigma L_s i_{qs}^{e}\right)^2 + \left(\omega_e L_s i_{ds}^{e}\right)^2 \le V_{s\_\max}^{\;2} \tag{9}$$

This voltage limit boundary is an ellipse which is the function of the operating frequency, ω_e, and the center of the voltage limit ellipse is the origin in the synchronous reference frame current plane. At the low speed region, the voltage limit ellipse is large enough, and the voltage can not be a constraint. However, as the operating frequency increases, the size of the voltage limit ellipse decreases, and the voltage becomes the constraint above the certain speed. To satisfy the voltage limit constraint in the flux weakening region, the current trajectory should be inside the voltage ellipse at every operating point as shown in Fig. 5.

Besides, in the electrolytic capacitor-less inverter, the maximum allowable stator voltage varies even under the same speed and load torque condition due to the fluctuation of the DC-link voltage as mentioned in (1) and (2). Therefore, to maximize the developed torque, it is preferred to exploit the fluctuating DC-link voltage in the electrolytic capacitor-less inverter as much as possible.

The second constraint is the current limit. The current boundary is limited by the machine rated current, $I_{s\_\max}$. Hence, the current limit can be formulated as (10).

$$i_{ds}^{e\,2} + i_{qs}^{e\,2} \le I_{s\_\max}^{\;2} \tag{10}$$

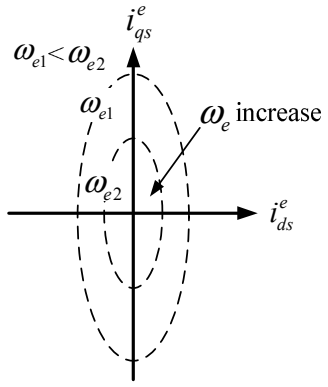

Fig. 5 Voltage limit ellipse in synchronous reference frame current domain

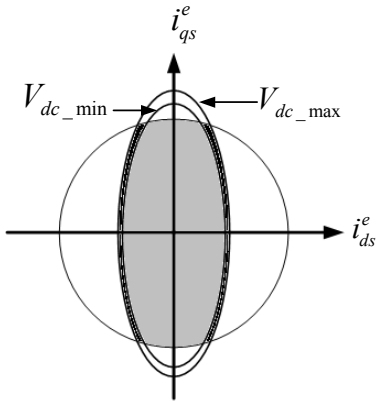

Fig. 6 Voltage limit ellipse and current limit circle of electrolytic capacitor-less inverter in synchronous reference frame current domain

As shown in (10), the center of the current limit circle is also the origin in the synchronous reference frame. The radius of the current limit circle is dependent on the maximum current of the machine. To satisfy the current constraint, the currents should be inside current limit circle at every operating point.

To satisfy the both voltage and current constraints, the currents trajectory should be inside the common area of a current limit circle and a voltage limit ellipse. In Fig. 6, the shaded area demonstrates the available currents region according to the DC-link voltage when utilizing the electrolytic capacitor-less inverter. As shown, there are two voltage limit ellipse due to the fluctuation of DC-link voltage. Too conservatively, if the voltage limit is restricted only by the small ellipse corresponding to $V_{dc\_\min}$, the developed torque would be small. Too radically, if only large ellipse corresponding to $V_{dc\_\max}$ is used as a voltage limit, the current would not be regulated due to the shortage of the voltage to the machine. Therefore, it is demanded to measure exactly the DC-link voltage and to reflect the voltage fluctuation to the flux weakening operation in real time.

IV. Proposed Flux Weakening Strategy

To regulate the currents in the flux weakening region, the output voltages of current regulator should be equal to the demanded voltages, which are given in (5) and (6). If the current is not regulated properly due to the lack of voltage margin in the flux weakening region, the current references should be modified, and the developed torque would be reduced. Hence, it is the major issue how to modify the current references to maximize the torque in the flux weakening operation.

Also, the flux weakening controller and anti-windup algorithm conflict as shown in [12]. And it is recommended to eliminate the anti-windup algorithm in the flux weakening operation. Therefore, the proposed flux weakening strategy only utilizes the flux weakening controller without any anti-windup function.

In this paper, the cost function is set to maximize the voltage utilization and to reduce the d-axis current reference in the synchronous reference frame appropriately. With the reduced d-axis current reference, the rotor flux in the synchronous reference frame, λ_{dr}^e, can be controlled for the flux weakening operation and the current regulation performance can be maintained. The proposed cost function to maximize the voltage utilization can be set as (11).

$$J = \frac{1}{2}\left(\Delta v_{ds}^{e\,2} + \Delta v_{qs}^{e\,2}\right) \tag{11}$$

And the voltage differences, Δv_{ds}^e and Δv_{qs}^e, are defined as (12) and (13).

$$\Delta v_{ds}^e = -\omega_e \sigma L_s i_{qs}^e - v_{q,\lim} \tag{12}$$

$$\Delta v_{qs}^e = \omega_e L_s i_{ds}^e - v_{q,\lim} \tag{13}$$

where $v_{d,\lim}$ and $v_{q,\lim}$ is the d and q-axis maximum realizable voltage in the synchronous reference frame.

In (12) and (13), although the maximum realizable voltage is fluctuating due to the small capacitance of the utilized electrolytic capacitor-less inverter, it can be considered as a constant value because the sampling frequency of the current regulation loop is much higher than the line voltage frequency. In the constant torque region, the voltage differences are usually zero because the voltage margin is sufficient. However, in the flux weakening region, the over-modulation usually occurs due to the increase of the demanded machine voltage. Therefore, the voltage difference appears at each operation point of the flux weakening region and the current reference should be modified at the operating point to resolve the difference.

The amount of modified d-axis current reference which minimizes the voltage difference can be calculated as (14).

$$\begin{bmatrix} \frac{d i_{ds}^{e}}{dt} \\ \frac{d i_{qs}^{e}}{dt} \end{bmatrix} = -\begin{bmatrix} \alpha_1 & 0 \\ 0 & \alpha_2 \end{bmatrix} \Delta J$$

$$= -\begin{bmatrix} \alpha_1 & 0 \\ 0 & \alpha_2 \end{bmatrix} \begin{bmatrix} \frac{\partial J}{\partial i_{ds}^{e}} \\ \frac{\partial J}{\partial i_{qs}^{e}} \end{bmatrix} \tag{14}$$

$$= -\begin{bmatrix} \alpha_1 & 0 \\ 0 & \alpha_2 \end{bmatrix} \begin{bmatrix} 0 & \omega_e L_s \\ -\omega_e \sigma L_s & 0 \end{bmatrix} \begin{bmatrix} \Delta v_{ds}^{e} \\ \Delta v_{qs}^{e} \end{bmatrix}$$

In (14), α_1 and α_2 are the proportional gains which decide the performance of flux weakening operation. The large proportional gain means poor voltage utilization. In order to increase the voltage utilization, it is better to set the small proportional gain. However, the smaller proportional gain means the larger current ripples due to the lack of voltage margin in the current regulation. By integrating the above equation, the amount of current modification can be obtained. However, to circumvent the offsets problem which may result in the divergence of the amount of current modification term, the low pass filter, whose cut-off frequency is around several Hz, can be used instead of the pure integrator. By above revision, the amount of current references modification can be deduced as (15).

$$\begin{bmatrix} \Delta i_{ds}^{e} \\ \Delta i_{qs}^{e} \end{bmatrix} = -\begin{bmatrix} \alpha_1 & 0 \\ 0 & \alpha_2 \end{bmatrix} \begin{bmatrix} \frac{\omega_1}{s+\omega_1} & 0 \\ 0 & \frac{\omega_2}{s+\omega_2} \end{bmatrix} \begin{bmatrix} \omega_e L_s \Delta v_{qs}^{e} \\ -\omega_e \sigma L_s \Delta v_{ds}^{e} \end{bmatrix} \tag{15}$$

Finally, the modified current references in the flux weakening region can be described as (16) and (17).

$$i_{ds,m}^{e} = i_{ds}^{e*} + \frac{1}{s+\omega_1}\left(-\alpha_d \omega_e L_s \Delta v_{qs}^{e}\right) \tag{16}$$

$$i_{qs,m}^{e} = i_{qs}^{e*} + \frac{1}{s+\omega_1}\left(\alpha_q \omega_e \sigma L_s \Delta v_{ds}^{e}\right) \tag{17}$$

where $i_{ds,m}^{e}$ and $i_{qs,m}^{e}$ is the modified d and q-axis current reference in the flux weakening region, i_{ds}^{e*} and i_{qs}^{e*} is the d and q-axis current reference in the constant torque region, and α_d and α_q is the proportional gain $\left(\alpha_d = \alpha_1 \omega_1, \alpha_q = \alpha_2 \omega_2\right)$, respectively.

The magnitudes of the modification part of the current reference increase as the voltage differences increase, which means the deep flux weakening operation.

From (16), the d-axis current reference in the synchronous reference frame can be obtained for the flux weakening operation. However, in order to maintain the torque, the q-axis current reference of (17) should be replaced as (18).

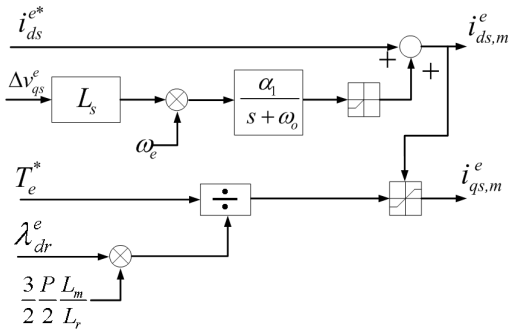

Fig. 7 Block diagram of the proposed current references generation scheme in the flux weakening region

$$i_{qs,m}^{e} = \frac{T_e^*}{\frac{3}{2}\frac{P}{2}\frac{L_m}{L_r}\lambda_{dr}^{e}} \tag{18}$$

where T_e^* is the torque reference.

In (18), the rotor flux in the synchronous reference frame can be obtained by using a closed-loop Gophinath flux observer which is presented in [13] or by using simple relation as (19) [14].

$$\lambda_{dr}^{e} = \frac{L_m}{\frac{L_r}{R_r}s+1} i_{ds,m}^{e} \tag{19}$$

Also, in order to satisfy the current limit condition, the q-axis current reference of (18) should be modified as (20).

$$i_{qs,m}^{e} = \min\left(\frac{T_e^*}{\frac{3}{2}\frac{P}{2}\frac{L_m}{L_r}\lambda_{dr}^{e}}, \sqrt{I_{s\_\max}^{2} - i_{ds,m}^{e\,2}} \right) \tag{20}$$

Fig. 7 shows the block diagram of proposed current references generation in the flux weakening region. In Fig. 7, there are two limiters. In case of an induction machine, the d-axis current reference in the synchronous reference frame should be positive to produce the rotor flux. Hence, a limiter is needed to avoid the situation where d-axis current in the synchronous reference frame is down below zero. And the q-axis current reference should be limited to keep the maximum current rating according to the modified d-axis current reference.

V. EXPERIMENTAL RESULTS

Table.1 shows the parameters of an induction machine under the test and Table.2 demonstrates those of the electrolytic capacitor-less inverter.. In this paper, LC filter with the damping resistor is used as the input filter where L_f is the inductance, C_f is the capacitance, and R_f is the parallel resistance of the input filter. As shown, the capacitance in the DC-link, C_{dc}, is only 9μF and the total capacitance only is 22.5μF which is less than 0.5 % of conventional PWM VSI. Fig.8 shows photos of the utilized electrolytic capacitor-less inverter and the control circuit. The size of electrolytic

TABLE I
NOMINAL PARAMETER OF A MOTOR UNDER THE TEST

Quantity	Value [Unit]
Rs	0.568[Ω]
σLs	8.04[mH]
Lm	88.6[mH]
Rr	0.374[Ω]
Pole pair	2
Rated power	7.5[kW]
Rated voltage	380[V_{rms}]
Rated current	19.2[A]
Rated speed	1730[r/min]

TABLE II
PARAMETERS OF ELECTROLYTIC CAPACITOR-LESS INVERTER

Quantity	Value [Unit]
Input Filter Inductance, L_f	200[μH]
Input Filter Capacitance, C_f (delta-connected)	9[μF] each
Input Filter Resistance, R_f	2.5[Ω]
DC Link Capacitance, C_{dc}	9[μF]

capacitor-less inverter is similar to the conventional PWM VSI without the dynamic braking resistor.

To see the performance of the proposed flux weakening strategy, the induction machine under the test is operated in torque control mode and the load machine which is directly coupled to the test machine, is operated in a speed control mode.

Fig. 9 is the experimental result when the induction machine is at 2000r/min with full load, where the induction machine operated in flux weakening region. In Fig.9, 'I_a' is the 'a' phase input current and 'V_{dc}' is the DC-link voltage. As shown, the DC-link voltage is fluctuating at 6 times of input frequency and 'a' phase input current is quasi-square wave.

Fig. 10 demonstrates the current regulation performance of the proposed flux weakening strategy. In Fig.10, i_{ds}^e, i_{qs}^e, and ω_{rpm} is the d and q-axis current in synchronous reference frame and the mechanical rotor speed, respectively. In Fig.10(a), the induction machine is operated at the motoring mode and it is accelerated from 1500r/min to 2000r/min at full load when the proportional gain, α_d, is set to -0.03. As shown in the figure, the d-axis current in the synchronous reference frame decreases to reduce the rotor flux, while q-axis current increases to maximize the developed torque when the rotor speed increases. In Fig.10(b), the induction machine is decelerated from 2000r/min to 1500r/min. As the operating point of induction machine is changed, the currents are modified to maximize the voltage utilization.

Fig.11 depicts the current regulation performance at generating mode. In Fig.11, the proportional gain is -0.03 and

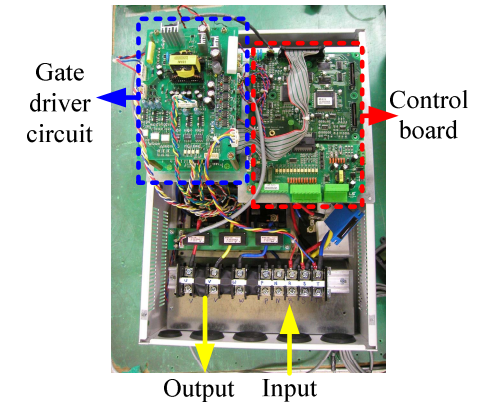

(a) control circuit

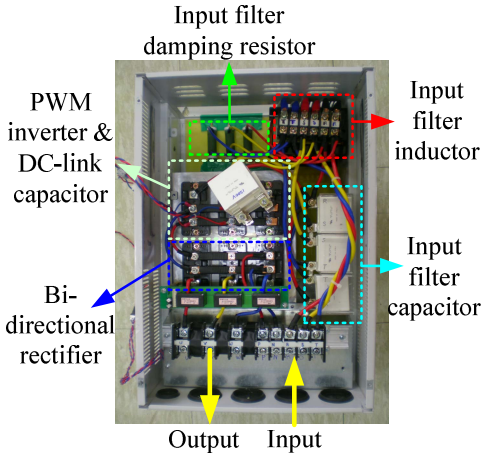

(b) power stack

Fig. 8 Prototype electrolytic capacitor-less inverter

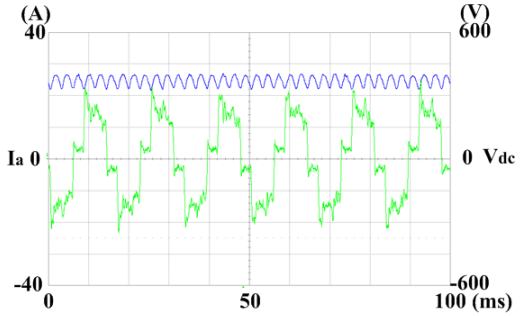

Fig. 9 Input current and sampled DC-link voltage at 2000 r/min

the induction machine is accelerated at full load from -1500r/min to -2000r/min and decelerated from -2000r/min to -1500r/min. The modification of currents is performed well without unstable point. In Fig.10 and Fig.11, although there is some oscillation in the d-axis current, the modified q-axis current has less oscillation with the consideration of the rotor time constant. From Fig.10 and Fig.11, it can be concluded that the proposed flux weakening strategy is acceptable under fluctuating DC-link voltage.

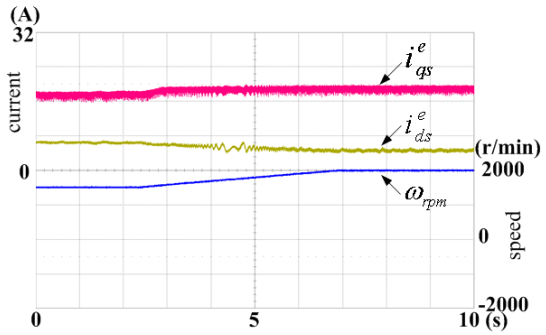

(a) from 1500r/min to 2000r/min

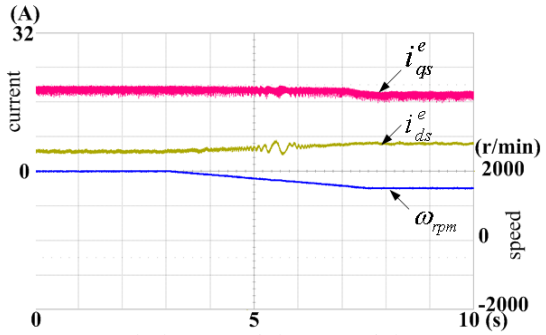

(b) from 2000r/min to 1500r/min

Fig. 10 Current of proposed flux weakening at motoring mode

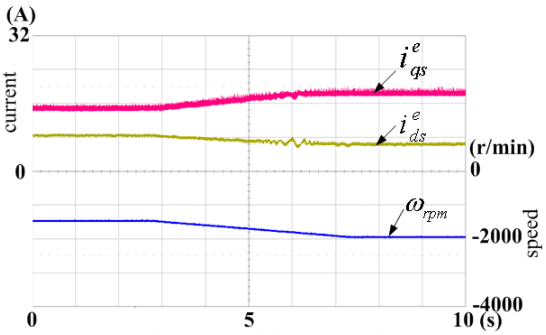

(a) from -1500r/min to -2000r/min

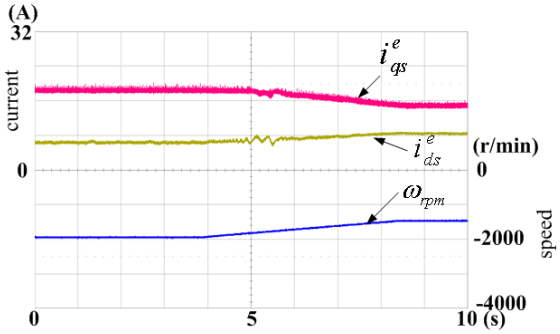

(b) from -2000r/min to -1500r/min

Fig. 11 Current of proposed flux weakening at generating mode

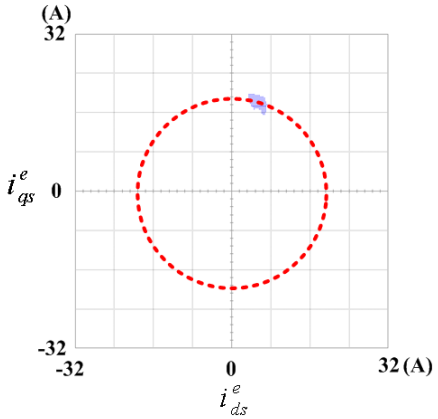

Fig. 12 Current trajectory of proposed flux weakening in the synchronous reference frame current domain

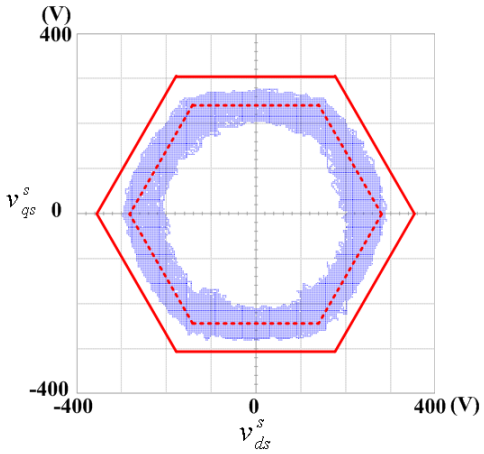

(a) The proportional gain is set as -0.03.

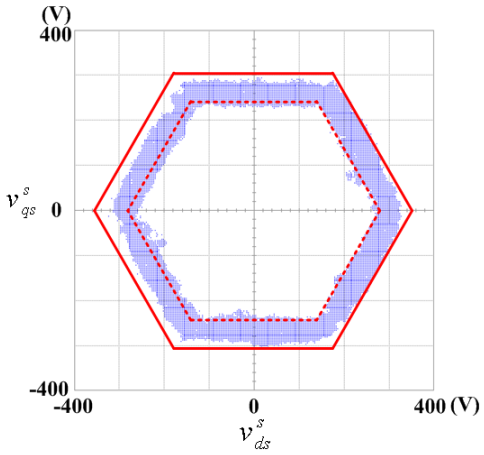

(b) The proportional gain is set as -0.003.

Fig. 13 voltage trajectory in the stationary voltage reference frame at 2000r/min

Fig.12 shows the current trajectory. The red dot circle means the current limit circle. As shown, the currents are on the current limit circle to maximize the developed torque.

Also, Fig.13 shows the d and q-axis voltage trajectory in the stationary reference frame. In Fig.13, v^s_{ds} and v^s_{qs} is the d and q-axis voltage in the stationary reference frame. The red solid line is the voltage limit hexagon considering the maximum value of the DC-link voltage and the red dot line is the one reflecting the minimum DC-link voltage. And the blue dots, which look like cloud, are the actual the voltage

references at each sampling instant when the induction machine is operated at 2000 r/min. In Fig.13 (a), the proportional gain, α_d, is set as -0.03 and in Fig.13(b), it is set as -0.003. When the proportional gain is smaller, the more voltage can be used. However, it is unavoidable to bring about the larger current ripple when the gain is smaller. Although the relatively small voltage is used with the large proportion gain, the magnitude of synthesized voltage is larger than the hexagon of the minimum DC-link voltage. From Fig.13, it can be seen that the proposed flux weakening strategy exploits the DC-link voltage maximally regardless of the continuous fluctuation of DC-link voltage. However, the available voltage to the machine varies according to the proportional gain, but still the voltage is above the hexagon set by $V_{dc\_\min}$.

VI. CONCLUSIONS

In the case of the electrolytic capacitor-less inverter, there is no reactive component in the DC-link except several μF film capacitor. Due to its small capacitance, THD of the input currents improved remarkably compared to that of the conventional PWM VSI. However, the DC-link voltage is fluctuating, and it is difficult to operate the induction machine properly in the flux weakening region.

In this paper, a novel flux weakening strategy of an induction machine driven by an electrolytic capacitor-less inverter is proposed to maximize the voltage to the induction machine in the flux weakening region. The proposed flux weakening strategy modifies the current references to exploit the DC-link voltage maximally. The experimental results have been shown to verify the feasibility and superiority of the proposed strategy. Though the available voltage to the machine varies according to the proportional gain, but still the voltage is above the hexagon set by $V_{dc\_\min}$.

REFERENCES

[1] Military Handbook 217 F, "Reliability prediction of electronic equipment," Revision F,Dec. 1991, Notice 1, July, 1992, Notice 2, Feb.1995.

[2] S. Kim, S.K. Sul, and T.A. Lipo, "AC/AC Power Conversion Based on Matrix Converter Topology with Unidirectional Switches," *IEEE Trans. on Industry Applications,* vol. 36, no. 1, pp. 139-145, 2000.

[3] M. Hinkkanen and J. Luomi, "Induction Motor Drives Equipped With Diode Rectifier and Small DC-Link Capacitance," *IEEE Trans. on Industrial Electronics,* vol. 55, no. 1, pp. 312-320, Jan, 2008.

[4] M. Alakula and J.E. Persson, "Vector Controlled AC/AC Converters With a Minimum of Energy Storage," *in Conf.Rec-IAS,* vol. 2, pp. 1130-1134, Oct, 1994.

[5] L. Malesani, L. Rossetto, P. Tenti and P. Tomasin, "AC/DC/AC PWM Converter with Reduced Energy Storage in the DC Link," *IEEE Trans. on Industry Applications,* vol. 31, no. 2, pp. 287-292, Mar/Apr, 1995.

[6] J.S. Kim and S.K. Sul, "New Control Scheme for AC-DC-AC Converter Without DC Link Electrolytic Capacitor," *in Conf.Rec.IEEE-PESC,* pp. 300-306, Jun, 1993.

[7] M. Hinkkanen, L. Harnefors and J. Luomi, "Control of Induction Motor Drives Equipped With Small DC-Link Capacitance," *in Conf.Rec.IEE-EPE*, Sep, 2007.

[8] S.H. Kim, and S.K. Sul, , "Maximum Torque Control of an Induction Machine in the Field Weakening Region," *IEEE Trans. on Industry Applications,* vol. 31, pp. 787-794, 1995.

[9] X. Xu, and D.W. Novotny, , "Selection of the Flux Reference for Induction Machine Drives in the Field Weakening Region," *IEEE Trans. on Industry Applications,* vol. 28, no. 6, pp. 1353-1358, Nov/Dec, 1992.

[10] A.Yoo, W.J.Lee, S.Kim, B.M.Dehkordi and S.K.Sul, "Input filter analysis and resonance suppression control for electrolytic capacitor-less inverter," *in Conf.Rec.IEEE-APEC,* pp. 1786-1792, Feb, 2008.

[11] B.Piepenbreier and L.Sack, "Regenerative Drive Converter with Line-Frequency Switched Rectifier and without DC Link Components," *in Conf.Rec.IEEE-PESC,* pp. 3917-3923, 2004.

[12] G.Y. Choi, M.S. Kwak, T.S. Kwon and S.K. Sul, "Novel Flux-Weakening Control of an IPMSM for Quasi Six-Step Operation," *IEEE Trans. on Industry Applications,* pp. 1722-1731, Nov/Dec, 2008.

[13] P.L.Jansen, and R.D.Lorenz, "A Physically Insightful Approach to the Design and Accuracy Assessment of Flux Observers for Field Oriented Induction Machine Drives," *IEEE Trans. on Industry Applications,* vol. 30, pp. 101-110, Jan/Feb, 1994.

[14] S.K.Sul, Electric Machine Control Theory, 2nd ed, Seoul, Korea, Hongneung Science Publication Co., 2007.